Recent advances of QWIP development in Sweden

Henk Martijn, Sergiy Smuk, Carl Asplund, Hedda Malm, Andrey Gromov,
Jörgen Alverbro, Henry Bleichner

IRnova, Electrum 236, 164 40, Kista, Sweden;

ABSTRACT

The ongoing development of QWIP focal plane arrays at IRnova (formerly Acreo) has resulted in the launch of several new formats up to 640 by 512 pixels and the introduction of major improvements to all products. The achieved performance and imagery will be evaluated. In the light of the development of new formats, the results of hybridization a 640 by 512 detector with 20 μm pitch will be discussed. The driving forces behind these improvements have been the demands from both industrial applications where the requirements for the operating temperature are high due to the life time issues, and from space applications where the requirements for the quantum efficiency and dark current are extreme. For the latter type of applications a number of QWIPs covering the 4 to 20 μm wavelength band have been grown and evaluated. The demands for better performance are met by ongoing increases in light coupling, improvements of the quantum well structures, as well as fine tuning of the epitaxial growth parameters. This has led to FPAs that can operate at 75 K and operation close to 80 K is within reach. IRnova is also looking at other material systems to fulfill the requirements of next generation photon detectors.

Keywords: QWIP, Infrared detectors, quantum well, dark current, photoconductive gain, antimonide, type II superlattice, LWIR

1. INTRODUCTION

The demands on future IR-detectors can be summarized according to:

- Higher operational temperature for the detector
- Higher sensitivity and shorter integration time
- Smaller pixels
- Higher resolution, meaning a greater amount of pixels
- Broad banded spectral response within LWIR-window (8-12 μm)
- Lower manufacturing cost

These sometimes conflicting requirements can only be achieved if all the available tools are used in a comprehensive optimization including all the aspects of the design and manufacturing of QWIPs. Band engineering should be combined with light coupling simulations to accomplish higher operating temperatures and better sensitivity. Improved growth techniques acquired in the quest for ultra low dark currents can also be applied for more conventional LWIR detectors.

In this work some of the activities and ideas employed to achieve the aforementioned requirements with QWIPs are presented.

2. IMPROVEMENTS

The working temperature of QWIPs (Quantum Well Infrared Photon detectors) has always been considered as a weak point compared to other detector technologies like MCT (Mercury-Cadmium-Telluride). A working temperature of 65 K or even lower is not uncommon for QWIPs operating in the LWIR band. The dark current is exponentially dependent on the temperature while the response remains basically unchanged. As it has been lined out in [1], response is linear dependent on the doping concentration whereas the dark current depends exponentially on this parameter. If a decrease of the doping concentration is balanced by an increase of the photoconductive gain, the dark current will be reduced whilst the response is held constant or even improved.

The present work shows the improvements achieved with the optimization of doping concentration in a modified bound-to-quasicontinuum structure (type 'B') with improved photoconductive gain as compared to the standard bound-

Infrared Technology and Applications XXXIII, edited by Bjørn F. Andresen, Gabor F. Fulop, Paul R. Norton,
Proc. of SPIE Vol. 6542, 65420V, (2007) · 0277-786X/07/$18 · doi: 10.1117/12.721700

Downloaded From: http://spiedigitallibrary.org/ on 06/17/2013 Terms of Use: http://spiedl.org/terms

tominiband structure (type 'A'). Furthermore, improvements to the physical shape and dimensions of the pixels are included in the type 'B' devices.

Further process development allowed for increasing the fill factor of the FPAs. A fill factor of 92 % was achieved. However, the effect of this improvement is by far greater than simple increase of the active area of the pixel. Larger area allowed for placement of an extra row and column of the 2D grating dots. This led to a significant improvement of the light coupling, which was estimated from simulations to be approximately 30 %. The contribution of the increased active area of the pixel is about 9 %.

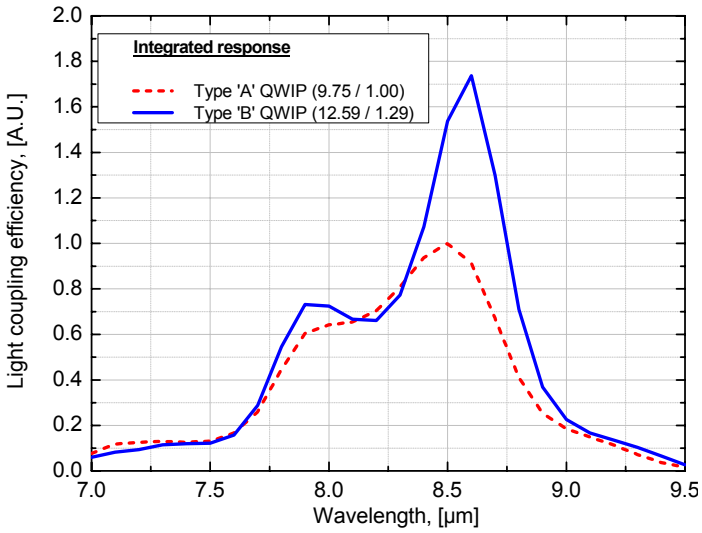

Figure 1. Light coupling efficiency for different fill factors.

In addition to the increased fill factor, an optimization of the layer structure of the FPA was performed. The optimization was targeted at increasing the light coupling efficiency and reducing the reflection of the light from the front surface of the detector. The reduced reflection makes the use of antireflective coating for QWIP FPA obsolete, which would contribute to the simplification of the manufacturing process and reduction of the manufacturing costs.

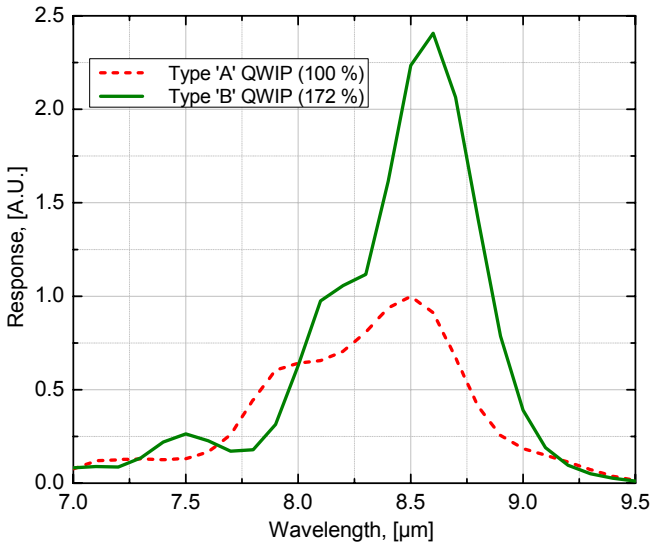

Figure 2. Improvements of the light coupling efficiency for different geometries of QWIP.

The total effect of the suggested improvements was estimated as more than 70 % according to the 3D finite element simulations.

Downloaded From: http://spiedigitallibrary.org/ on 06/17/2013 Terms of Use: http://spiedl.org/terms

This improved structure has been used in two types of FPA's, a 640 by 480 pixels large format and a 384 by 288 pixels mid format detector.

Table 1. FPA information and test conditions.

	QWIP640	**Sesam384**
Format	640 by 480 pixels, 25 μm pitch	384 by 288 pixels, 25 μm pitch
Readout	Argus640, IRnova's own readout	ISC0208, Indigo's readout
Well capacity	24×10^6 electrons	18.5×10^6 electrons
Noise	2900 electrons	850 electrons
F-number	2.7	2.7

Please note the much higher noise level of Argus640 readout as compared to the ISC0208.

Table 2. Results of evaluation of QWIP640 FPA

Detector	**Detector structure**	**Detector temperature**	**NETD**	**Dark current** (percentage of full well)	**Integration time**
QWIP640 F/2.7	type 'A'	65.0 K	29.1 mK	14 %	10.4 ms
QWIP640 F/2.7	type 'B'	65.0 K	25.9 mK	4 %	7.1 ms
QWIP640 F/2.7	type 'B'	70.0 K	30.3 mK	18 %	5.7 ms
QWIP640 F/2.0 (predicted)	*type 'B'*	72.5 K	39.3 *mK*	29 %	4.6 *ms*

The improved type 'B' structure shows that operation at 70 K gives basically the same NETD compared to the type 'A' structure at 65 K, whereas the integration time is almost half of that of the type 'A' structure. When an aperture of F/2 is used a satisfactory performance with an NETD just above 40 mK can be expected.

Figure 3. An image taken with a QWIP640 camera (courtesy of FLIR Systems AB, Danderyd).

Downloaded From: http://spiedigitallibrary.org/ on 06/17/2013 Terms of Use: http://spiedl.org/terms

Table 3. Results of evaluation of Sesam384 FPA.

Detector	Detector structure	Detector temperature	NETD	Integration time
Sesam384 F/2.7	type 'B'	70.0 K	27.0 mK	4.40 ms
Sesam384 F/2.7	type 'B'	73.5 K	37.9 mK	3.65 ms
Sesam384 F/2.7	type 'B'	75.0 K	51.8 mK	2.90 ms

The measurement results for the Sesam384 FPA show marginally better performance as compared to the QWIP640 FPA. The higher readout noise of the latter FPA does not have a significant influence on the performance because the major noise sources are the photon noise and generation-recombination noise of the dark current.

2.1 Quantum Well Density

In addition to the optimization of doping concentration and photoconductive gain in the band structure we performed an experimental series for optimization of the quantum well density. The aim of these experiments was to find an optimal number of quantum wells keeping the thickness of entire detector pixel constant.

There are three major contributions to the dark current: thermionic emission, thermally assisted tunneling, and temperature-independent direct interwell tunneling [2,3]. Results of the experiment series show that the interwell tunneling component of the dark current is smaller than the thermal components for the 40-periods structure at 60K temperature and higher, see Figure 4.

The dark current balance for this structure looks similar to that of the 30-periods variant at the same working temperature. That means that at a temperature of 60 K and higher 40 periods can be used instead of 30 without producing higher dark current. The response remains unchanged, however a larger number of quantum wells results in a higher quantum efficiency.

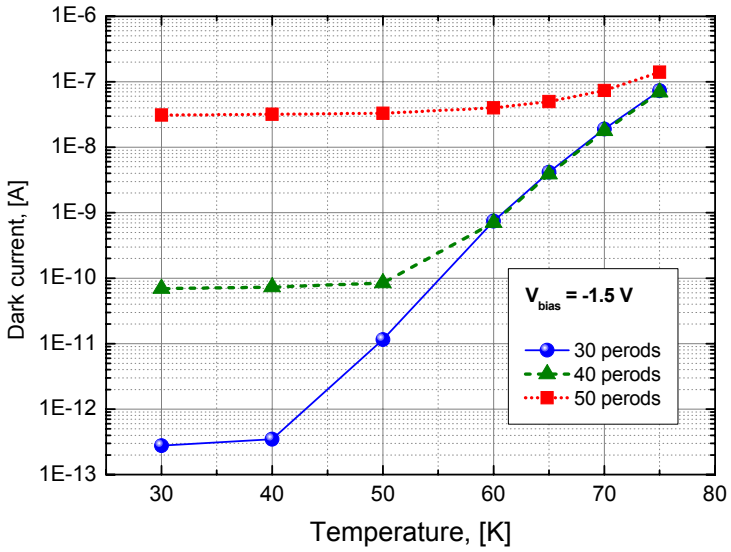

Figure 4. The dark current in the test structures with different quantum well density at different temperatures, bias voltage -1.5V.

3. NEW FORMATS

QWIP FPAs with smaller pixels are developed due to the continuously increasing demand for arrays with higher resolution (pixel count) and the price level of systems. Smaller pixels allow for smaller FPA and thus for smaller IDDCA (Integrated Detector Dewar Cooler Assembly) and systems, which in turn will have an impact on the power dissipation and weight of the system. The major two obstacles are the producibility (the hybridization process becomes increasingly

Downloaded From: http://spiedigitallibrary.org/ on 06/17/2013 Terms of Use: http://spiedl.org/terms

difficult the smaller the pixels are) and the light coupling into the pixel, which is crucial for QWIPs because of its polarization sensitivity of absorption. This is normally accomplished with a 2D grating converting the normally incident light into absorbable state [4-6]. The grating becomes however less effective for smaller pixels, simply because fewer grating dots fit on one pixel. This light coupling efficiency is simulated with a full 3D finite element simulation. Results of such simulation are presented in Figure 5. The coupling efficiency drops quite drastically for smaller pixels. However the efficiency of a 20 µm pixel is still at the acceptable level of 86 % of the efficiency of a 25 µm pixel.

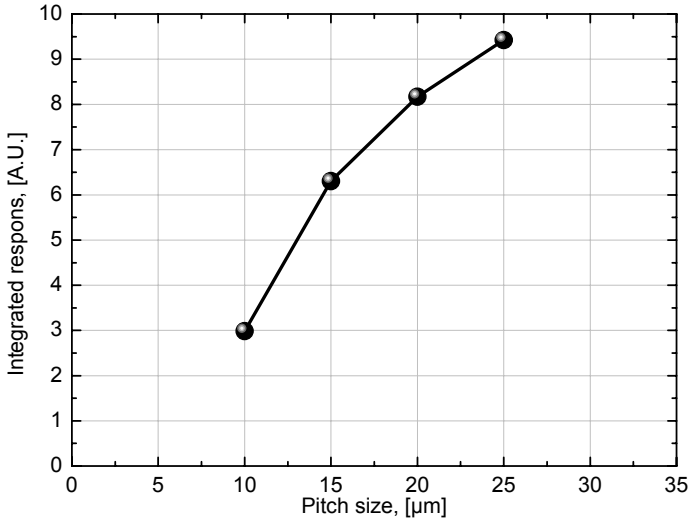

Figure 5. Results of 3D finite element simulation of the light coupling efficiency as function of pixel size.

These results can be used to predict the performance of an FPA with 20 µm pixels.

Table 4. Performance prediction for a detector with 20 µm pixel (well capacity: 1.1×10^6 electrons; noise: 700 electrons; F-number: 2.7)

Detector temperature	**NETD**	**Dark current** (percentage of full well)	**Integration time**
65.0 K	*28.1 mK*	*7 %*	*8.4 ms*
70.0 K	*39.7 mK*	*26 %*	*6.5 ms*
72.5 K	*55.3 mK*	*41 %*	*4.9 ms*

Due to the worse response to dark current ratio the performance is not quite as good as QWIP640 or Sesam 384 but still acceptable at 70 K.

3.1 Hybridization

Flip-chip bonding is done with a SUSS MicroTec FC150 flip-chip bonder. Cold compression of indium bumps is used as bonding process. An under-bump metal (UBM) and indium bumps are therefore deposited on both the detector and ROIC prior to flip-chip bonding. Indium is deposited by a thermal evaporator. Before the flip-chip bonding can start the flip-chip bonder is calibrated with our own calibration process. This has led to a very good operational yield for our QWIP640 FPA.

Last year (2006) work commenced on the hybridization of 640×512 pixel detectors with 20µm pitch. The results are very promising with high yield and operability. The operability statistics is shown in Figure 6. In total, 69 hybridizations have been performed. The median operability for the series is 99.84 %.

Downloaded From: http://spiedigitallibrary.org/ on 06/17/2013 Terms of Use: http://spiedl.org/terms

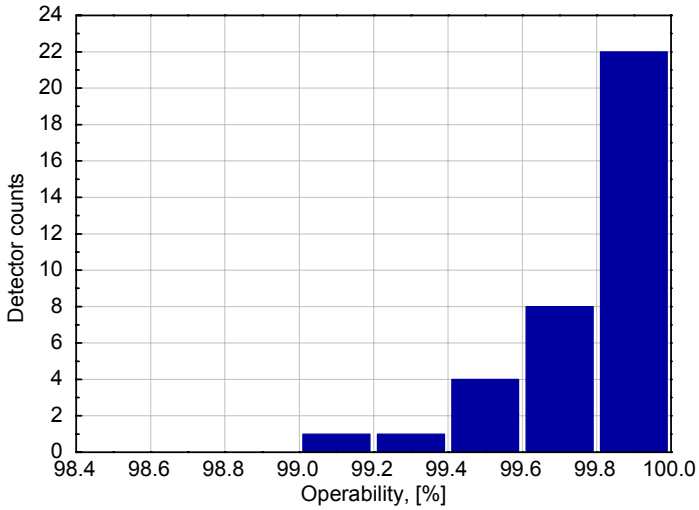

Figure 6. Operability statistics for 640 by 512 detectors with 20 μm pitch hybridized at IRnova in 2006-2007.

The QWIP-detectors are thinned down in a two-step process after flip-chip bonding. First, the major part of the GaAs substrate is removed by a mechanical step. The second step is to remove the reminder of the GaAs substrate and only leave the epitaxial structure. This is done in a wet etch process. There is an ongoing work to automate and speed up the thinning down process with equal or better yield.

The thinning down is done for several reasons, primarily to minimize mechanical stress when detector is cooled down but also to minimize the cross-talk and improve the optical coupling.

4. SPACE APPLICATIONS

4.1 Growth temperature

An important factor, which determines the ultimate performance of AlGaAs/GaAs QWIP structures for space applications, is the concentration of detrimental (*n*-type) impurities in the barriers. The latter, especially deep states from Si, are known to increase the dark current and must thus be avoided. This is especially important in space applications, where a combination of long detection wavelengths and low background conditions put stringent requirements on the detector dark current characteristics.

The detectors structure is grown with MOVPE (Metal Organic Vapor Phase Epitaxy).

Regardless of the source of Si (reactor contamination, gas impurities, etc.) its incorporation in the AlGaAs barriers can be hindered to some extent by lowering the temperature of the epitaxial growth. This has been confirmed by secondary-ion mass spectroscopy (SIMS) profiles through multilayer structures, which show that a growth temperature reduction from 710 to 650 °C gives 2-3 times smaller Si background doping in AlGaAs.

QWIP structures for the VLWIR range fabricated using two different growth temperatures confirm that the reduced growth temperature, and thus reduced Si background doping in the AlGaAs barriers, is beneficial for the dark current. The dark current characteristics for the two structures are given in Figure 7. However, the interpretation of the results needs some discussion, since the sample grown at 650 °C accidentally has a slightly longer cutoff-wavelength (i.e. lower barrier height). We observe the following:

- Despite the longer cutoff, the 650 °C sample has smaller dark current at T < 25 K.
- For temperatures over 25 K, however, the dark current increases much faster in the 650 °C sample, than in the sample grown at 710 °C.

As argued below, we interpret this as an evidence that the 650 °C sample has barriers of higher purity, and that the thermal component of the tunneling current, and thus also the barrier height, become increasingly important as the temperature is raised.

Downloaded From: http://spiedigitallibrary.org/ on 06/17/2013 Terms of Use: http://spiedl.org/terms

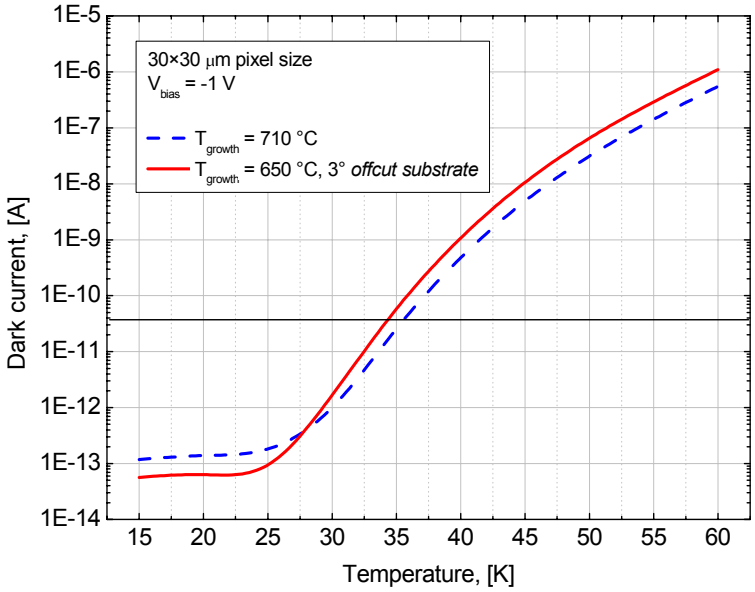

Figure 7. Dark current characteristics for two VLWIR QWIP structures with peak response around 14 μm. For these particular structures the transition between the two regimes of temperature-dependent and temperature-independent behavior occurs around 25 K.

The dark current vs. temperature curve of a QWIP detector can be divided into a temperature-independent and a temperature-dependent regions, see Figure 7. The former occurs at low temperatures where only a very small fraction of the electrons have energies close to the barrier edge. Impurity states (from e.g. Si doping) in the barriers are of great importance in this case, since their presence effectively enhance the probability for tunneling. In this temperature range the dominating dark current mechanism is impurity-assisted dark current and not thermally-assisted tunneling. In other words, the barrier purity is a more important parameter for influencing the magnitude of the dark current than the exact barrier height.

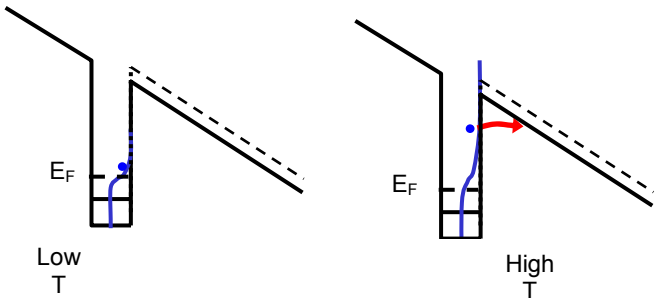

Figure 8 A schematic illustration of the energy distribution for the two dark current regimes.

In the second, temperature-dependent temperature range, a certain fraction of the electrons in the QW ground state has sufficiently high energy to tunnel through the barrier. This is the normal operating regime for commercial LWIR or MWIR QWIP applications. Already a small increase $+\delta V$ of the barrier height gives a significant reduction of the total tunneling probability (= dark current). This is due to the overlap of the barrier edge with the smeared energy distribution of the QW ground state (high energy tail). For the same reasons small changes of the detector temperature δT will also have a great effect on the dark current in this temperature range.

Whereas the effect of barrier impurities completely dominates the dark current in the temperature range of temperature-independent behavior, it is still an important factor to be considered at higher temperatures. The impurity states (typically more than 50 meV deep in the case of Si) simply enhance the electron tunneling probability through the barriers by

Downloaded From: http://spiedigitallibrary.org/ on 06/17/2013 Terms of Use: http://spiedl.org/terms

offering alternative tunneling paths, so a sample with such impurities in the barriers will always have higher dark current at *all* temperatures, than a similar sample without the impurities.

The practical implications are that a reduced growth temperature will reduce dark current also for the conventional LWIR QWIP structures.

5. NEXT GENERATION LWIR, ANTIMONIDE BASED TYPE II SUPERLATTICE

Infrared detectors based on Type II InAs/GaSb superlattices have the potential to reach higher operating temperatures and better responsivity than current QWIPs [7-10]. There are known challenges with high leakage currents, specifically currents on the surface of the mesas. Before tackling these difficulties with different types of surface treatments and passivations, the design and properties of the detector material it self have to be investigated.

An epitaxial structure is grown with MBE (Molecular Beam Epitaxy) on 2" GaSb substrate. It is designed for LWIR (cutoff 10µm) and consists of thin layers of InAs/GaInSb. The structure is a *p*-*i*-*n* diode with the *p*-contact of GaSb closest to the substrate following by the *p*-doped, undoped (intrinsic or weak *n*-type) and *n*-doped superlattice layers. The structure is finished with *n*-contact of InAs. Rather large (155 µm by 155 µm) single pixel devices have been processed and evaluated.

5.1 Results

The structure has been analyzed with TEM (Transmission Electron Microscopy) not only to asses the material quality but also to make out what the type of interface between the different materials was (Figure 9). The type of the interface is of utmost importance to get the right electrical-optical behavior.

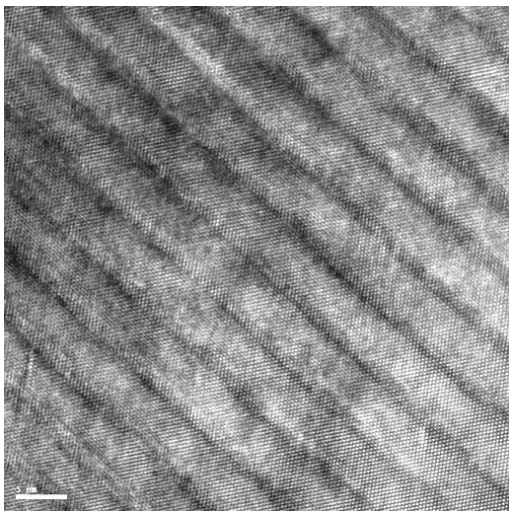

Figure 9. TEM micrograph of the Type II InAs/GaSb superlattice test structure. The scale marker in the lower left corner corresponds to 5 nm in the image. The growth direction is from the lower left to the upper right corner.

A TEM image shows that the material quality was very good and had the right number of InAs and GaInSb monolayers. On the other hand it was not possible to identify the type of the interface.

The superlattice detector has, as opposed to QWIPs, a wide band response. The first responsivity measurements can be seen in Figure 10a. At 65 K and almost 0 V bias the peak responsivity is 0.62 A/W (at 6.15 µm). At 80 K the peak responsivity was measured at 0.51 A/W. This can be compared with a detector with a cutoff at ~8 µm and responsivity of 2-3 A/W at 77 K and 0 V bias, as published in [11].

In Figure 10b, the dark current for different temperatures is shown.

Downloaded From: http://spiedigitallibrary.org/ on 06/17/2013 Terms of Use: http://spiedl.org/terms

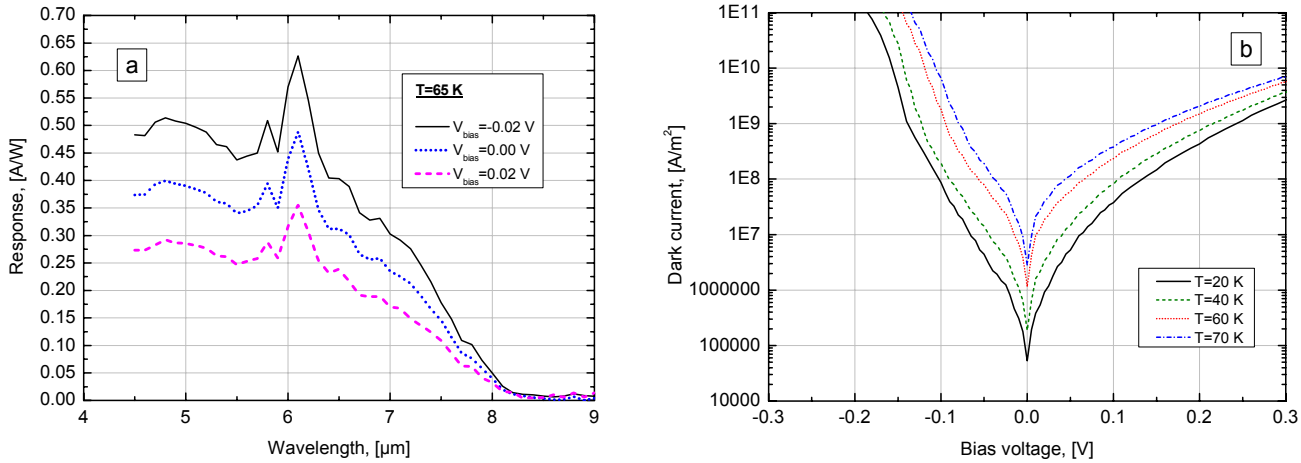

Figure 10. Experimental results for the SbSL test structure evaluation: *a* – responsivity at 65K; *b* – dark current at different temperatures.

The structure was designed with a responsivity cutoff around 10 μm. The measurements show however a cutoff closer to 8 μm. The hypothesis is that the type of interface between InAs and GaInSb is not correct and thus the strain in the structure differs from the design value, which in its turn means that the band structure is not correct. This hypothesis will be tested in the future.

6. SUMMARY

- By optimizing the trade-off between the doping concentration and optical gain and by improving the geometric design of the mesa, the operating temperature has been increased by 5 K and the integration time reduced by a factor of 2.
- The electro-optical simulations of 20 μm pixels lead to a predicted performance of less than 40 mK NETD at 70 K operating temperature. The next step will be to validate this experimentally.
- Very good results have been achieved with the hybridization of 640 by 512 detectors with 20 μm pixels with median operability of 99.84 %.
- A way to improve the material quality has the potential to lower the dark current for LWIR detectors.
- The first results of antimonide-based type II superlattice are very promising with responsivity already higher than that achieved with QWIPs.

7. ACKNOWLEDGEMENTS

The work was partly performed under contracts 16427/02/NL/JA, 18264/04/NL/PA and 19575/05/NL/IA granted by ESA/ESTEC to Acreo. Part of the work was also financially supported by FLIR Systems AB, Sweden, and FMV - Swedish Defence Material Administration. The authors would like to thank all the personnel of IRnova for their efforts in performing this work.

Downloaded From: http://spiedigitallibrary.org/ on 06/17/2013 Terms of Use: http://spiedl.org/terms

8. REFERENCES

1. A. Gromov, C. Asplund, S. Smuk, H. Martijn, "Optimisation of QWIP performance for high temperature and low background applications", Proc. of SPIE vol. 6395, pp. 639502 (2006).
2. Andrews S.R. and Miller B.A. "Experimental and theoretical studies of the performance of quantum-well infrared photodetectors", J. Appl. Phys., Vol.70, p.993 (1991).
3. Williams G.M. et al., "Excess tunnel currents in AlGaAs/GaAs multiple quantum well infrared detectors", Appl. Phys. Lett., Vol.60, p.1324, (1992)
4. J. Y. Andersson and L. Lundqvist, "Near-unity quantum efficiency of AlGaAs/GaAs quantum well infrared detectors using a waveguide with a doubly periodic grating coupler", Appl. Phys. Lett, 59, p. 857-859 (1991).
5. J. Y. Andersson and L. Lundqvist, "Grating coupled quantumwell infrared detectors: Theory and performance", J. Appl. Phys. 71, p. 3600-3610 (1992)
6. L. Lundqvist, J. Y. Andersson, Z. F. Paska, J. Borglind, and D. Haga, "Efficiency of grating coupled AlGaAs/GaAs quantum well infrareddetectors", Appl. Phys. Lett.,63, p.3361-3363 (1993).
7. R.H. Miles and D.H. Chow in Long wavelength infrared detectors, edited by M. Razeghi (Gordon and Breach Science Publishers, Amsterdam, 1997), pp. 397-451
8. M. Walther, J. Schmitz, R. Rehm, S. Kopta, F. Fuchs, J. Fleiβner, W. Cabanski, J. Ziegler, Journal of Crystal growth 278, p. 156-161 (2005).
9. F. Fuchs, Ahlswede, M. Walther, J. Wagner, P. Koidl, "High performance InAs(GaIn)Sb superlattice infrared photodiodes" Appl. Phys. Lett. 71, p. 3251 (1997)
10. R. H. Miles and J. A. Wilson, "GaInSb/InAs Type-II Superlattices for 10 μm IR Detector Applications", Electrochemical Society Proceedings Vol. 95-28, p. 195-199 (1995).
11. M. Razeghi, "Type II InAs/GaSb superlattices for high-performance photodiodes and FPAs2, Proc. of SPIE vol. 5246, pp. 501-511 (2003).

Downloaded From: http://spiedigitallibrary.org/ on 06/17/2013 Terms of Use: http://spiedl.org/terms